Electronic Materials Letters, Vol. 6, No. 4 (2010), pp. 215-220
DOI: 10.3365/eml.2010.12.215 Published 31 December 2010

Response Improvement of Integrated Humidity Sensors Using a Micropump

Sung Pil Lee*

Department of Electronic Engineering, Kyungnam University, Masan-si, Gyeongnam 631-701, Korea

An integrated humidity sensor system with micropumps was fabricated, and its pumping capability and response characteristics were investigated. The suitability of valve-less micropumps in the sensor system was demonstrated through a simple micromachining process using deep reactive ion etching (DRIE) and an anodic bonding step. The Reynolds number of the pump with a diffuser angle of 19° is about 1200, and the maximum flow rate is 0.176 μl/min. The optimum resonant frequency is 100 Hz for water and 600~800 Hz for air. The sensitivity of the humidity sensor system with pumping is 10 times higher than it is without pumping for repeated refresh cycles.

Keywords: micropump, integrated humidity sensor, DRIE, CMOS, response time

1. INTRODUCTION

Chemical microsensors such as measuring probes, when they are in an unknown medium, identify a specific component and determine its concentration within the medium. Such a component can be toxic gases within the exhaust system of a motor vehicle or water molecules in the air of a room. The sensors must not have any cross-sensitivities, i.e., the values they measure must not change when other substances are present. They must also respond rapidly in order to regulate the combustion process optimally or to indicate a malfunction. Most of chemical sensors require a settling-down time during which the system reaches equilibrium, also known as the response time. The resulting response time may be immediate or it may require the sensor system to reset after each measurement, reaching its base equilibrium state before being used with the next sample. Too long a time, however, can materially affect the usefulness of the method for repetitive routine analyses. However, with sensors of a chemical or biochemical nature, this response time is greatly offset by the simplicity of the measurement and by minimal sample preparation times. For a chemical sensor, the goal is to minimize the power and/or temperature necessary for operation because a low temperature is favored for power consumption and safety. In particular, oxide semiconductor gas sensors and humidity sensors at room temperature, however, have a disadvantage in that those types show relatively slow response times.[1,2] Therefore, many researchers have worked to develop devices that show high sensitivity and fast responses to species of interest at room temperature.[2-5]

Microfluidic handling modules are necessary in microanalysis systems to transport samples, chemicals, and reference media. These modules typically consist of micropumps and microvalves which can be controlled individually depending on their applications. Valveless micropumps should be simple and inexpensive to make. They can either be mechanical or non-mechanical. Mechanical systems contain moving parts usually associated with their actuation, such as valve membranes or flaps. The driving force can be generated by utilizing piezoelectric, electrostatic, thermo-pneumatic, pneumatic or magnetic effects. Piezoelectric actuators are widely used in valveless reciprocating micropumps. Because valveless micropumps that utilize piezoelectric disks have a simple structure and no internal moving parts, there is less risk of clogging the valves when pumping fluids that contain particles. Valveless micropumps also allow for a smaller device size.[6-7]

In this paper, we apply the CMOS-MEMS technique to fabricate an integrated humidity sensor system with a micropump to improve the response time. A silicon-based valveless micropump actuated by a piezoelectric disc which is attached onto the sensor chip is designed to realize a feasible inlet/outlet size ratio of the diffuser and to reduce the capillary pressure caused by bubbles in the pump chamber. The response of the humidity sensor system is discussed with and without pumping.

2. DESIGN AND FABRICATION

The integrated humidity sensor system consists of a differential-type FET sensor, a Wheatstone bridge sensor, a diode temperature sensor, a Hall sensor and a built-in heater. The

*Corresponding author: sensors@kyungnam.ac.kr

chip size is 9.0 mm × 5.4 mm with 30 pins. The layout and a photograph of the humidity sensor system are shown in Fig. 1. The differential-type FET configuration consists of two sensing FETs and two reference FETs. The peripheral shadow area over the heater is the bonding space for the micropump. Reference transistors are applied to eliminate the effect of unwanted factors, such as the temperature, other gases or electrical noise. The fabrication is based on 0.8 ìm CMOS technology utilizing two poly, two metal, poly silicon/nitride etch stop in conjunction with twin-well process. For the formation of the sensing materials on the gate layer, plasma etching is conducted on each gate with a trench. Sensing materials are deposited by a reactive RF magnetron sputtering system with a DC bias and are patterned by a lift-off technique. Carbon nitride film for the humidity-sensing materials is then applied.[8,9] To fulfill the requirement of a differential sensor, a gas-permeable gold layer is deposited only onto the gate region of the sensing transistor. Photo resist material for passivation is coated on the gate area of the reference FETs to prevent a reaction with the gas.[10]

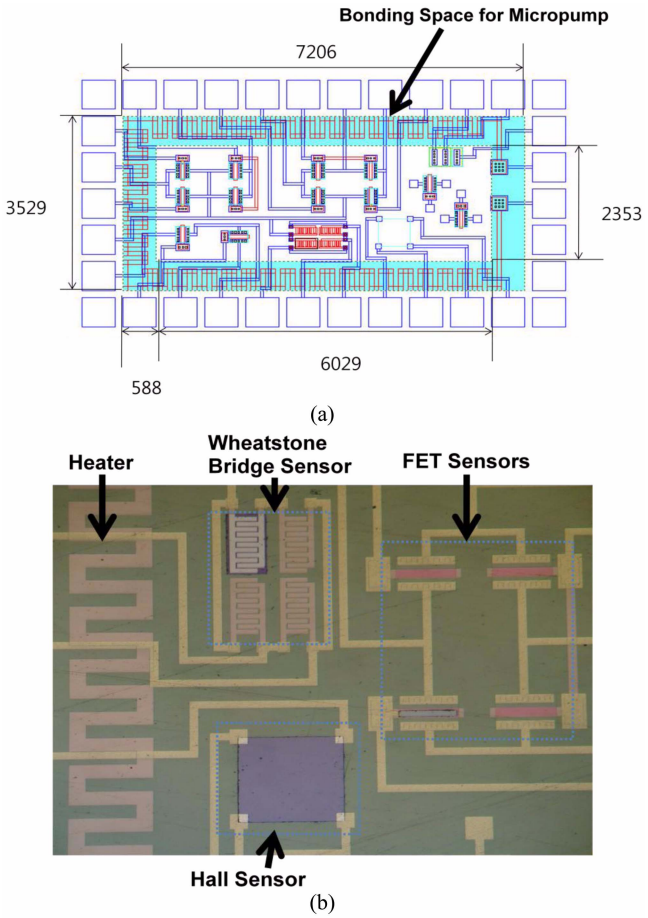

Fig. 1. Design and fabrication of sensor system: (a) a layout of the integrated sensor system attachable with the micropump and (b) a photograph of the chip after post-processing.

The valveless diffuser micropump for the pumping of both gas and liquid was designed and fabricated. Diffusers usually have circular or rectangular cross-sections. They are known as conical diffusers and flat-walled diffusers, respectively.[7,11] In this study, the diffuser/nozzle has a flat-wall with a w_1 distance of 400 μm. Additionally, w_2 varied at 400 μm, 600 μm, 800 μm and 1000 μm. Fig. 2 shows the layout and a photograph of the micropump in which w_1 is 400 μm and w_2 is 600 μm. When the diffuser length is L= 1200 μm, the cone angle 2θ is respectively 0°, 19°, 38° and 54° given the varying w_2 values above. The height of the diffuser/nozzle element is 350 μm, as determined by the thickness of the etched layer out of which it is microfabricated. Hence, the cross-sectional areas of the inlet and outlet of the diffuser/nozzle are determined by $S_1 = 1.4 \times 10^{-7}$ m^2 and $S_2 = 1.4 \times 10^{-7}$ m^2~3.5×10^{-7} m^2, respectively. The fabrication of the micropumps is accomplished through a very simple MEMS process involving only two subsequent DRIE steps on the front side of a (100) p-type silicon wafer. During the first etching process, the inlet and outlet are created at the diffuser and nozzle. The resist mask is removed, and the membrane is formed in the second etch. A piezoelectric disc (Piezotechnology, PIC 255) with a thickness of 0.2 mm and a size of 4.5 mm × 2 mm is glued on using conductive epoxy on the diaphragm. Hence, the micropump is anodically bonded in a prepared oxide space in the integrated humidity sensor system.

3. MEASUREMENTS

The pump characteristics were assessed for their ability to

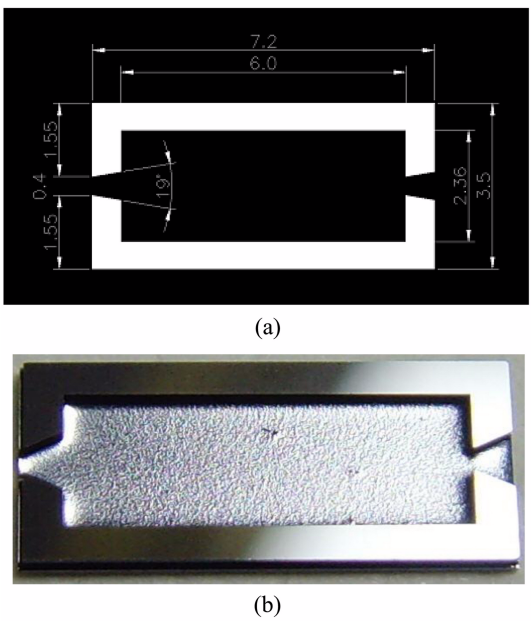

Fig. 2. Micropump for integrated sensor system: (a) a layout of the valveless micropump with diffuser angle of 19° and (b) a microscope image of DRIEed silicon diaphragm and diffuser/nozzle.

handle liquids and gases. Colored water was injected into the pump cavity after a methanol treatment to minimize the risk of a gas bubble becoming trapped in the cavities of the pump. The methanol treatment makes pump filling easier as methanol has a much lower surface tension than water.[7] The micropump was mounted onto an acrylic resin plate with a hole under a standard microscope, as shown in Fig. 3. The driving pulse of the piezoelectrical disc was applied using a photo coupler to prevent electrical breakdown, and an IGBT (Insulated Gate Bipolar Transistor) was used to ensure that the resonant frequency remained in the range of 1 Hz to 1 kHz. Depending on the pump flow, the volume flow was calculated by the displacement of the liquid in a tube with a known diameter (1 mm). The micropump attached onto the integrated humidity sensor system was put in a constant-temperature chamber controlled by a PID controller to measure the response time of the sensor. To regulate the humidity, dry air and water-saturated air controlled by a mass-flow controller were introduced into the measurement chamber at a flow rate of 25 sccm.

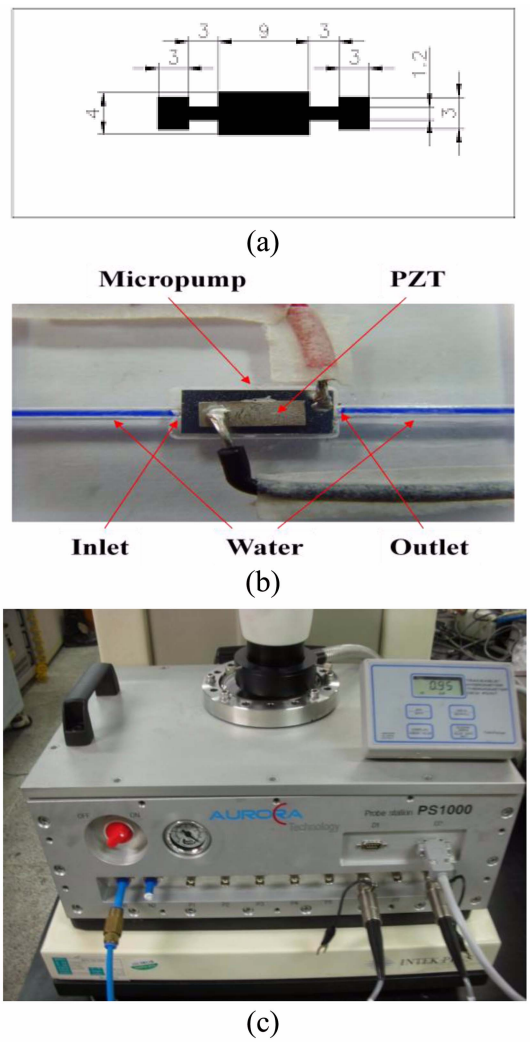

Fig. 3. Measurement of micropumps: (a) a designed acrylic plate, (b) displacement measurement of water by the micropump, and (c) a measurement chamber with the temperature/humidity controller.

4. RESULTS AND DISCUSSION

Valveless micropumps have a relatively simple structure in comparison with micropumps with check valves or active valves. The geometrical parameters of the diffuser are key elements in valveless micropumps. Fig. 4 shows the displacement variation for the width ratio between the inlet and the outlet, w_1/w_2, in a single-chamber micropump with a flat-walled diffuser/nozzle. In this work, the slenderness, which is defined as the length divided by the neck width of the diffuser inlet, is 3. The Reynolds number that provides the measurement of the ratio of the inertial forces to the viscous forces is defined as follows:

$$R_e = \frac{\overline{\mu_1} L}{v} \tag{1}$$

where, $\overline{u_1}$ is the mean fluid velocity, L is the travel length of the fluid and v is the kinematic viscosity. When all calculations are done in two dimensions using water as the fluid ($v = 1.0 \times 10^{-6}$ m^2/sec), Re=1200 for $\overline{u_1} = 1$ m/s.[12] The slenderness and the Reynolds number are lower than other results reported earlier.[11,12] The earlier studies indicated a slenderness that higher than 13 and a Reynolds number typically higher than 5000. The micropump in this study had to follow the CMOS design rules because the micropump is positioned on the bonding space in which silicon dioxide is grown on a built-in heater of the integrated humidity sensor system. Hence, the diffuser/nozzle length L is determined as the heater width. The built-in heater plays role in resetting the sensors rapidly during the desorption process. If the heater is designed to be larger to increase both the slender-

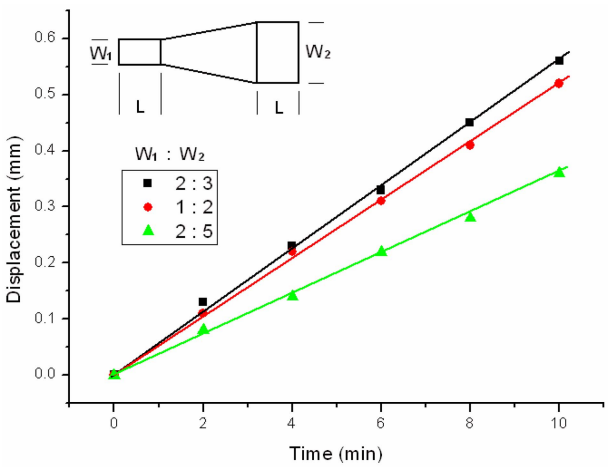

Fig. 4. The displacement of water as a function of time for different diffuser dimensions.

ness and the Reynolds number of the micropump, a considerable amount of time would be required for heat dissipation to return to its normal state. The micropumps for the humidity sensors do not require a great amount of pumping ability to manage the flow of the gases; a fast flow rate can disturb the adsorption process of water molecules on the adsorption sites of the sensor. The diffuser, however, must work in the transitory steady stall region and not in the bi-stable steady or jet flow region. The pressure loss coefficients of the diffuser and the nozzle can be written, respectively, as follows:

$$K_d = \frac{\Delta p_d}{\rho \bar{u}^2_{w_1}/2} \tag{2}$$

$$K_n = \frac{\Delta p_n}{\rho \bar{u}^2_{w_2}/2} \tag{3}$$

where, Δp_d is the pressure drop in the diffuser direction, Δp_n is the pressure drop in the nozzle direction and ρ is the fluid density. The diffuser element efficiency ratio can be defined by the equation below.

$$\eta = \frac{K_n}{K_d} \tag{4}$$

To achieve $\eta > 1$, the nozzle-diffuser element has to be conical with a rounded inlet and a sharp outlet.[11] The pumping characteristics for pumps with different width ratios of 2: 3, 1: 2 and 2: 5 show linear behavior. The maximum flow rate is 0.176 μl/min at a width ratio of 2:3 (a diffuser angle of 19°). The flow rates are much lower than the values reported earlier owing to the small slenderness and Reynolds number values, as mentioned before.[7,11-13]

One of the important factors associated with reciprocating pumps that use the oscillatory movement of a membrane to displace fluids is the resonant frequency. Piezoelectric actuation is a very attractive concept, as it provides a comparatively high stroke volume, a high actuation force and a fast mechanical response. Moreover, commercial PZT material is readily available for hybrid integration. The operation of this pump utilizes a piezoelectric effect to excite the diaphragm at its first natural frequency. When the membrane is deflected upward in the first half-cycle (the supply mode), additional fluids would come into the chamber through the diffuser compared to those dropped through the nozzle. During the other half-cycle (the pump mode), the diffuser in the first half cycle serves as a nozzle when the membrane is deflected downward. Subsequently, additional fluid flows through the outlet. The resonant frequency, which is determined by the membrane stiffness (K_p) and the inertia of the fluid in the diffuser, can be expressed as

$$f_o = \frac{1}{2\pi}\sqrt{\frac{K_p(1+\sqrt{\eta})^2 h(w_1 - w_2)}{\rho K_v (1+\eta) L \ln(w_2/w_1)}} \tag{5}$$

where K_v is the ratio of the pumping chamber volume variation amplitude to the deflection of the membrane at the center. The optimum resonant frequency that has the highest flow rate is 100 Hz, as shown in Fig. 5. Yamahata *et al.*[12] reported that the resonant frequency of a PMMA micropump with electromagnetic actuation was 12 Hz for water and approximately 180 Hz for air, while Linnemann *et al.*[14] found that the optimal frequency was 200 Hz for water. The measured resonant frequency is in fairly good agreement with the other values, as the resonant frequency depends on the pump structure, materials and actuation method.

Carbon nitride film is a good candidate for use as a humidity sensing material due to several advantages related to this type of film. These include its facility compatibility with Si fabrication, its fast response time over a wide humidity range, its long-term stability against chemical contamination, and its low cost.[8] Unstable carbon nitride films can react with hydroxyl groups in moist air, causing the C≡N and/or C=N bonds to break and leading to the formations of C-H and N-H bonds. This can be explained by the action of the compressive stretching of hydrogen atoms and the tensile stretching of carbon atoms in the films after the reaction between hydrogen and the CN compound. When water molecules encounter carbon nitride permeating the porous gold layer of FET humidity sensors, they are chemisorbed on the available sites of the carbon nitride surface by a dissociative mechanism to form two hydroxyl ions for each water molecule, which possess a high local charge density and a strong electrostatic field. The proton reacts with an adjacent surface O^{2-} group to form a second OH^- group. When the first layer of water molecules is formed, a subsequent layer of water molecules is physically adsorbed on the first hydroxyl layer. The physisorbed water easily dissociates to form H_3O^+ due to the high electrostatic fields in the chemisorbed layer. The physisorption changes from a monolayer to a multi-layer

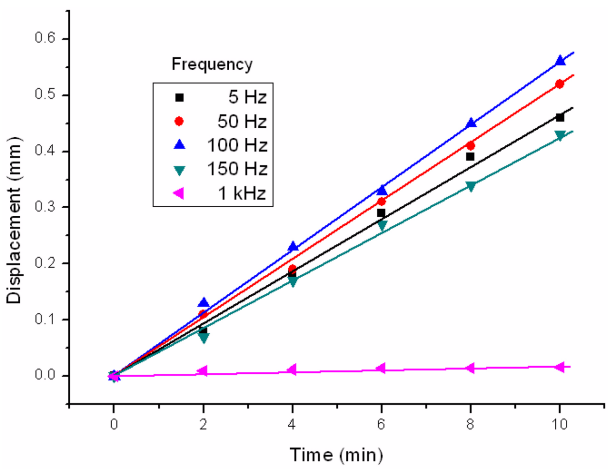

Fig. 5. The displacement of water as a function of time for different actuation frequencies.

structure as the water-vapor pressure increases. Water molecules in the succeeding physisorbed layer are only single-bonded and form a liquid-link network. Therefore, the single-bonded water molecules are able to form a dipole and reorient freely under an externally applied gate field, resulting in an increase in the dielectric constant. This is caused by an increase in the capacitances in sensing materials, which can be attributed to changes in the threshold voltage and increases in the drain current of the FET humidity sensors.[9,10] Despite the fact that FET drain currents have a wide range in which they can change, hysteresis exists as a consequence of the slow recovery of the desorption process. The hysteresis in the humidity sensors is caused by the ink-bottle-shaped pores which become wider in the interior than they are at the surface. The condensed water vapor in the pores cannot easily come out. The dynamic changes in the voltage across the sensor with and without pumping are shown in Fig. 6. The applied power of the pulse to activate the piezoelectrical disc was 700 mW, the width ratio of the diffuser/nozzle was 2:3, and the frequency was 700 Hz. The resonant frequency can be theoretically calculated by Pan's model.[15] Putting the various parameters of the designed micropump into Eq. 5, with $\rho = 1.3$ kg/m^{-3} for air, the resonant frequency was estimated to be 600 Hz to 800 Hz. Therefore, we applied the median of the resonant frequency range.

The adsorption time was measured to the 90% point of the final steady state value after an abrupt change in the relative humidity from 0% to 95%; however, the desorption time was defined as 40% of the saturated value after 95% RH to 0% RH for convenience of measurement. With pumping, the response time for adsorption and desorption improved by 7 s and 46 s, respectively.

The repeated response of the sensor is shown in Fig. 7. Three refresh cycles were applied in a time internal in which the sensor was exposed at a 95 % relative humidity level for 60 s, after 40 s, and in dry air for 180 s. A significant improvement was noted by pumping at the desorption speed compared to when pumping was not done. The sensitivity of the humidity sensors can be defined as

$$S(\%) = \frac{V_o - V_d}{V_o} \times 100 \quad (6)$$

where V_o is the saturated voltage and V_d is the voltage after desorption. The sensitivity of the humidity sensor system with the micropump was 10 times higher than it was without the micropump.

5. CONCLUSION

Micropumps, which were fabricated by a two-step DRIE process, were attached onto an integrated humidity sensor system to improve the response time. According to calculations that utilized the geometrical factors of the micropump, the resonance frequency was determined to exist in the frequency range of approximately 5 Hz to 130 Hz for water, whereas it was about 600 Hz to 800 Hz for air. Hence, when operating the micropumps, due to the low mobility, if water is used as a medium, congestion can occur in the chamber at a higher frequency. In contrast, if air is used as the medium, the flow operation is normal and much smoother, even at the higher frequency, due to the high mobility of air. When the proposed micropumps were applied to a humidity sensor system, it was easy to observe that operating the system with the micropumps resulted in better values; with pumping, the absorption time was faster by 7 s and the desorption time was faster by 46 s. This difference was much more dramatic showing nearly ten-fold increase in speed and much higher sensitivity upon repeated measurements.

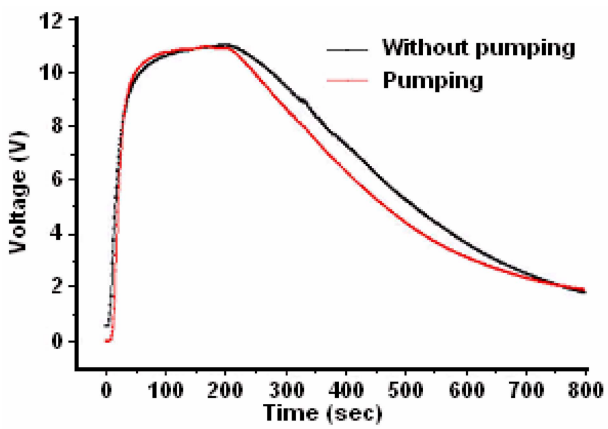

Fig. 6. Responses of the integrated humidity sensor with and without pumping.

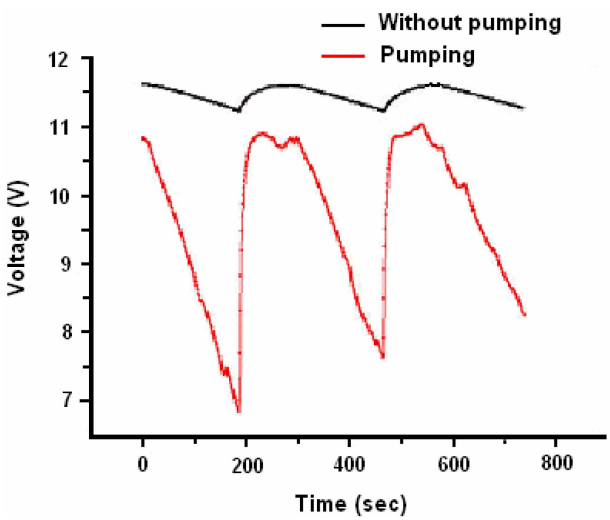

Fig. 7. Responses of integrated humidity sensor for 3 repeated refresh cycles.

ACKNOWLEDGMENT

This work was supported by Kyungnam University Foundation Grant 2009.

REFERENCES

1. G. S. Korotchenkov, S. V. Dmitriev, and V. I. Brynzari, Sensor. Actuat. B-Chem. **54**, 202 (1999).
2. U. Kang and K. Wise, IEEE Trans. Elect. Devices **47**, 702 (2000).
3. Z. M. Rittersma, A. Splinter, A. Bodecker, and W. Beneke, Sensor. Actuat. B-Chem. **68**, 210 (2000).
4. Y. Y. Qiu, C. Azeredo-Leme, L. R. Alcacer, and J. E. Franca, Sensor. Actuat. A-Phys. **92**, 80 (2001).
5. M. Burgmair, M. Zimmer, and I. Eisele, Sensor. Actuat. B-Chem. **93**, 271 (2003).
6. P. Woias, Sensor. Actuat. B-Chem.**105**, 28 (2005).
7. A. Olsson, P. Enoksson, G. Stemme and E. Stemme, J. Microelectromech. Sys. **6**, 161 (1997).
8. S. P. Lee, Electron. Mater. Lett. **5**, 1 (2009).
9. S. P. Lee, J. G. Lee, and S. Chowdhury, Sensors **8**, 2662 (2008).
10. S. P. Lee, Electron. Mater. Lett. **6**, 7 (2010).
11. V. Singhal, S. V. Garimella, and J. Y. Murthy, Sensor. Actuat. A-Phys. **113**, 226 (2004).
12. C. Yamahata, C. Lotto, E. Al-Assaf, and M. A. M. Gijs, Microfluid. Nanofluid. **1**, 197 (2005).
13. J. Fang, K. Wang, and K. Bohringer, J. Microelectromech. Sys. **15**, 871 (2006).
14. R. Linnemann, P. Woias, C. D. Senfft and J. A. Ditterich, Proc. MEMS '98, 25-29, 532, Heidelberg, Germany (1998).
15. L. S. Pan. T. Y. Ng, X. H. Wu, and H. P. Lee, J. Micromech. Microeng. **13**, 390 (2003).